# Ferromagnetic Polarons in Manganites

C.D. Batista

*Centro Atómico Bariloche and Instituto Balseiro, (8400) S. C. de Bariloche, Argentina.*

J. Eroles

*Centro Atómico Bariloche and Instituto Balseiro, (8400) S. C. de Bariloche, Argentina,*
*Los Alamos National Laboratory, Los Alamos NM 87545, USA.*

M. Avignon

*Centro Atómico Bariloche and Instituto Balseiro, (8400) S. C. de Bariloche, Argentina,*
*Laboratoire d'Etudes des Propriétés Electroniques des Solides (LEPES)*-CNRS - BP 166, 38042 Grenoble Cedex 9, France.*

B. Alascio

*Centro Atómico Bariloche and Instituto Balseiro, (8400) S. C. de Bariloche, Argentina.*
(July 21, 1999)

Using the Lanczos method in linear chains we study the double exchange model in the low concentration limit, including an antiferromagnetic super-exchange $K$. In the strong coupling limit we find that the ground state contains ferromagnetic polarons whose length is very sensitive to the value of $K/t$. We investigate the dispersion relation, the trapping by impurities, and the interaction between these polarons. As the overlap between polarons increases, by decreasing $K/t$, the effective interaction between them changes from antiferromagnetic to ferromagnetic. The scaling to the thermodynamic limit shows an attractive interaction in the strong coupling regime ($J_h > t$) and no binding in the weak limit ($J_h \simeq t$).

## I. INTRODUCTION

The discovery of 'colossal' magnetoresistance (CMR) [1] together with its many unusual properties has received considerable attention lately. The materials that exhibit this phenomenon are under much experimental investigation due to their technological applications. These perovskites are ferromagnetic oxides of the form $A_{1-x}B_x MnO_3$ (where A=La,Pr,Nd; B=Sr,Ca,Ba,Pb) [2,3]. Experiments have revealed very rich phase diagrams interpreted in terms of ferromagnetic, antiferromagnetic, canted, polaronic, and inhomogeneous phases. Charge ordered phases have also been found [4–9] in these compounds.

The phase diagram, as a function of concentration $x$, temperature, magnetic field, or magnitude of the relation between super-exchange and hopping interactions is not completely understood yet for the different compounds. A clear asymmetry is observed between hole ($x < 0.5$) and electron doped ($x > 0.5$) regimes. A metallic ferromagnetic phase can be reached by hole doping of the parent compound $LaMnO_3$, by substituting La for divalent alkalis, Pb, or by stoichiometry changes. On the other side, electron doped systems exhibit charge ordering or quasi-ordering and antiferromagnetism.

In the hole doped perovskites, the strong correlation between itinerant carriers and localized spins gives rise to competing magnetic interactions. This competing interactions plus the effects of disorder and lattice degrees of freedom, could give rise to inhomogeneities of varying scale: microscopic polarons, mesoscopic droplets or macroscopic phase separation. A number of experimental data indicating the different scales in the hole doped regime can be found in refs. [10,11] for polarons, [12] for droplets and [13] for phase separation.

Much less is known about the electron doped compounds. This lack of initial interest can be explained by the fact that manganites such as $Bi_{0.25}Ca_{0.75}MnO_3$ or $A_{0.25}Ca_{0.75}MnO_3$ are characterized by charge ordering phenomena and do not exhibit magnetoresistive effects. However the recent discovery of new ferromagnetic electron doped manganites, $Ca_{1-x}B_x MnO_3$ and $Ca_{1-x}Bi_x MnO_3$ for $x = 0.10$ [14,15], has increased the interest for those compounds since it opens the possibility of magnetoresistance effects also in this concentration limit. $Ca_{0.9}Bi_{0.1}MnO_3$ and $Ca_{0.9}Eu_{0.1}MnO_3$ exhibit indeed negative magnetoresistance but with a much smaller magnitude than hole doped manganites. Long range charge ordering has recently been observed with electron diffraction in $La_{1-x}Ca_x MnO_3$ ($x > 0.5$) [6–9,16,17]. The magnetic susceptibility has a pronounced inflection at the charge ordering temperature, resembling that associated with a conventional long range antiferromagnetic transition [18]. Neutron scattering measurements in $Bi_{1-x}Ca_x MnO_3$ ($0.74 < x < 0.82$) [9] indicate that charge ordering is accompanied by a structural transition and antiferromagnetic long range order indeed develops at lower temperature. The nature of spin fluctuations changes from ferromagnetic to antiferromagnetic at the charge ordering transition [9]. Optical reflectivity

studies of the same compound for $T_{co} > T > T_N$ have revealed the coexistence of a polaron response and a charge-gap-like structure in the optical response [8]. This two phases behavior is characterized by domains of ferromagnetic and antiferromagnetic spin correlations. Magnetization and resistivity measurements in $Ca_{1-x}Sm_xMnO_3$ for $0 < x < 0.12$ are interpreted in terms of the existence of a cluster glass metallic state below some critical temperature and demonstrate the lack of true ferromagnetism in these electron doped manganites [19].

From the theoretical point of view, the pioneering work of de Gennes [20] proposed a canted phase to resolve the competition between the ferromagnetic double interaction introduced by the presence of itinerant holes and the superexchange interaction. Recently, several contributions to this problem have been reported. Arovas and Guinea [21], studied this problem using a Schwinger boson formalism to obtain a phase diagram showing several homogeneous phases and pointing out that phase separation replaces the canted phase in a large region. Indeed phase separation appears in several numerical treatments of the problem [22]. In other analytical treatments, more adequate to treat local instabilities, non-saturated local magnetization states have appeared at zero temperature [23]. M. Yu. Kagan *et. al.* [24] have studied the stability of the canted phases against the formation of large ferromagnetic 'droplets' containing several particles and they conclude that the formation of droplets is favored in the ground state. The variety of results obtained from the different approaches points to the need of clarifying the picture and testing the results.

The diversity of results in the phase diagram is connected to the two dominant magnetic interactions acting in these systems: double exchange arising from the $e_g$ orbitals and antiferromagnetic superexchange due mainly to half-filled $t_g$ orbitals. These competing interactions could give rise to textures of different scales according to the relation between them.

Here we study a model for *diluted compounds* that characterizes them in terms of a single parameter: the relation between superexchange and hopping energies. In fact the ionic radii of the intervening dopants varies substantially the hopping matrix element through the variation of the Mn-0-Mn angle as discussed in ref. [25].

In this work, we find the low energy quasiparticles and characterize their structure and dispersion relation in the low concentration limit. These quasiparticles correspond to the electron followed by a ferromagnetic local distortion (ferromagnetic polaron) in the antiferromagnetic (AF) background. The dispersion relation is dominated by $k \to k + \pi$ scattering due to the presence of AF order. In order to make a connection with transport properties, we study the tendency to localization of these polarons in the presence of impurities and magnetic field.

We also study the interaction between the quasiparticles. For two particles, the profile of each quasiparticle is practically the same as the one obtained for only one particle. The effective magnetic interaction between these quasiparticles is antiferromagnetic for large values of $K$ and becomes ferromagnetic when the size of the polarons increase over some critical value. This change in the spin-spin correlation is followed by a change in the charge-charge interaction. If the size of the ferromagnetic distortion induced by one particle is larger than some critical value the other particle shares the same distortion giving rise to a bipolaronic bounded state.

We include diagonal disorder in the two particles problem in order to determine how this affects the effective interactions between the polarons. We find that randomness in diagonal energies induce a distribution of effective interactions between localized polarons which can be ferro or antiferromagnetic.

## II. THE MODEL

To render evident the nature of the ground state, we resort to the Lanczos method, which is free from approximations. The Hamiltonian is simplified to a single orbital per site, no lattice effects are considered, and we have to reduce to one dimensional chains. However our results provide a simple picture that, we presume, can put to test the dilute limit of electron doped systems. In these systems, the limitations of the model Hamiltonian may not be as stringent as in the hole doped systems for the following reasons: the lattice structure is more symmetric so Jahn Teller distortions should play a less important role. This observation is consistent with the fact that hole doped manganites $La_{1-x}Ca_xMnO_3$ are insulating for low concentrations of dopant while electron doped ones $Ca_{1-x}Sm_xMnO_3$ are semimetallic for similar values of $x$ [19]. The large in-site Coulomb repulsion inhibits double occupation so that it may be possible to describe the physics by the use of a single effective orbital, and finally the antiferromagnetic structure of two interpenetrating lattices can be properly described in one dimension.

In order to describe the manganites we consider two degrees of freedom: localized spins that represent the $t_{2g}$ electrons at the Mn sites, and itinerant electrons that hop from $e_{2g}$ $Mn$ orbitals to nearest neighbor $e_{2g}$ orbitals. The model Hamiltonian includes Hund coupling $(J_h)$ between localized and itinerant electrons, an antiferromagnetic superexchange interaction between localized spins $(K)$, a hopping term of strength $t$ which we will use as energy unit hereafter and an on site $(U)$ and nearest neighbor $(V)$ Coulomb repulsions:

$$H = -J_h \sum_i \mathbf{S}_i \cdot \sigma_i + K \sum_{<i,j>} \mathbf{S}_i \cdot \mathbf{S}_j \qquad (1)$$
$$+ \sum_{<i,j>,\sigma} t_{ij} \left( c_{i\sigma}^+ \cdot c_{j\sigma} + h.c. \right)$$

$$+V \sum_{<i,j>} n_i n_j + U \sum_i n_{i\uparrow} n_{i\downarrow}$$

where $n_{i,\sigma} = c_{i\sigma}^+ c_{i\sigma}$ ($n_i = n_{i\uparrow} + n_{i\downarrow}$), and $c_{i\sigma}^+$, $c_{i\sigma}$ creates and destroys an itinerant electron with spin $\sigma$ at site $i$, respectively. $\mathbf{S}_i$ and $\sigma_i$ are the localized and itinerant spin $1/2$ operators at site $i$, respectively. In order to reduce the Hilbert space we take S $=1/2$ for the localized spins instead of S $=3/2$. It has been shown numerically that, in the absence of antiferromagnetic coupling, the results for S $=3/2$ and $1/2$ are qualitatively similar [22]. This model has been studied numerically for finite concentration in reference [26], and in the absence of AF coupling ($K = 0$) in reference [22]. Recently some results have been obtained for a very small value of $K/t$ ($K/t = 0.05$) [27]. In this paper we focus on the dilute limit considering the cases of one and two added electrons.

In the following we will concentrate on the case $U = V = 0$, unless stated otherwise. It is believed for the manganites that the coupling $J_h$ is large. However there are some observations in LaMnO3 and CaMnO3 which indicate that $J_h$ could be not so large. Quoted values refer to $J_h = 1eV$ from optical conductivity data [28] and bandwidth $W = 1eV$ [5]. In our one dimensional counterpart model this would mean $Jh = 4t$. Band structure calculations [29] also indicate $Jh = 1eV$. A larger value of $Jh$ is inferred from scanning tunneling spectroscopy [30]Recent optical conductivity for CaMnO3 gives $1.7eV$ [31], and $2eV$ [32]. However $W$ is also larger in the ferromagnetic. Sarma et. al. [32] indicate $W = 4eV$ ($t = 0.3eV$), giving $Jh/W = 1/2$. In one dimension this would correspond to $Jh = 2t$. In all cases $U = 8 - 10eV >> Jh$. For that reasons we will keep the model general considering both the strong coupling ($Jh \sim 10eV$) and weak coupling ($Jh \sim 1eV$) regimes.

## III. ONE PARTICLE

In this section we investigate the homogeneity of the solutions for different values of $K/t$. To this end, we calculate the ground state with one itinerant $e_{2g}$ electron added for chains of different sizes up to $N = 20$. For large values of $J_h$, the particle modifies substantially the spin structure in its surroundings forming magnetic polarons. The distortions of the magnetic structure around the particle can be determined from correlation functions which mix charge and spin variables. In this way it is possible to distinguish between polaronic and non-polaronic regimes.

The quasiparticle character of this polaronic distortion becomes evident from the dispersion relation. The effective mass of the quasiparticle is inversely proportional to the bandwidth. In this way it is possible to study the variation of the effective mass as a function of the parameters.

By lowering the diagonal energy in one site it is possible to localize the polaron. We study the dependence of the localization length and the spin distortion on the effective mass and on an external magnetic field.

The correlations functions of this section have been calculated using periodic boundary conditions (PBC).

### A. Polaron profile

In order to determine the polaron profile we calculate $< n_i S_j S_{j+1} >$ for the ground state. Because of translation symmetry this correlation function depends only on $|i - j|$. The results for different values of $K/t$ and $J_h = 10t$ are shown in Fig.1($a$) where we plot $N < n_0 S_j S_{j+1} >$ vs $j$, where $N$ is the number of sites. As it can be seen in Fig.1, for large $j$ this correlation function takes a value very close to the one obtained from the Bethe ansatz solution of the Heisenberg chain, $< S_j S_{j+1} > \cong -0.443$. The extension and the magnitude of the spin distortion around the particle increases as $K/t$ decreases. By lowering the value of $K$, the system takes all the possible values of total spin $S$. This indicates that the size of the polaron increases continuously. It is clear from Fig.1 that the polaronic regime appears for $K < 0.3$.
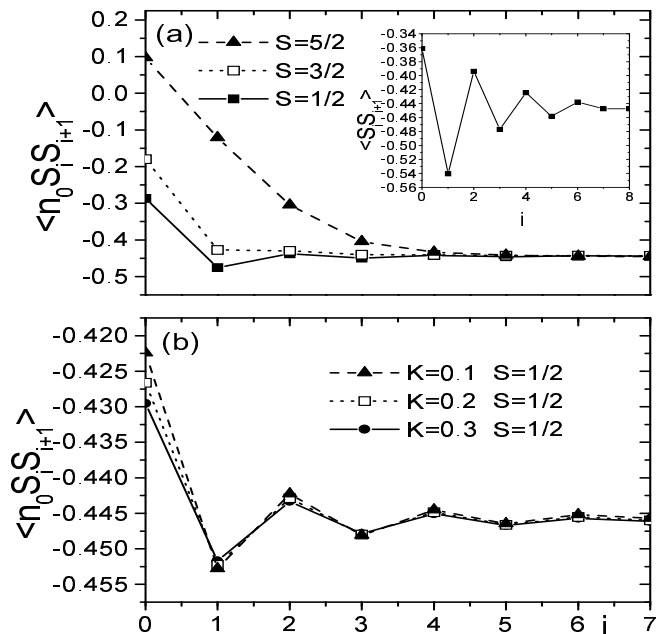
FIG. 1. *a*) We show the correlation function $< n_0 S_j S_{j+1} >$ for a 16 sites chain, with $J_h = 10$ and different values of $K$ ($K = 0.1$ triangles, $K = 0.2$ open squares and $K = 0.3$ full squares). The maximum value of $S$ for each value of $K$ is indicated in the figure. One can observe that the total $S$ and the extension of the magnetic distortion increase as $K$ decreases. The oscillatory behavior found at $K = 1$ is a consequence of the weakening of the antiferromagnetic links around the charge. The inset shows $< S_j S_{j+1} >$ for a 16 sites Heisenberg chain where the link at site zero is a factor 2 smaller than the rest. *b*) The same as *a*) for the weak coupling regime ($J_h = 1$).

In Fig.1(b), we show the same correlation function for $J_h = t$. For this value of $J_h$ we are already in the weak coupling limit where the spin distortion is almost null for any value of $K/t$ (notice the change in the vertical axis scale). The profile of the distortion in this case is, in fact, very similar to the one obtained in the strong coupling limit ($J_h \sim 10t$) for large values of $K/t$.

The oscillations observed in the curve corresponding to $K = 0.3$ are also observed for larger values of $K$. They are a consequence of the weakening of the antiferromagnetic links around the charge position which produce a sort of local spin dimerization. Because of the competence between double-exchange and super-exchange, the effective antiferromagnetic interaction between the site where the particle is and the nearest neighbor one is weakened ($\langle n_0 S_0 S_1 \rangle > -0.443$). The next spin correlation ($\langle n_0 S_1 S_2 \rangle$) may be even stronger than in the undoped case ($\langle n_0 S_1 S_2 \rangle < -0.443$) due to this weakening. This forces the next link ($\langle n_0 S_2 S_3 \rangle >$) to be weaker, and the same kind of reasoning can be applied to the rest. This effect explains the oscillations of $< n_0 S_j S_{j+1} > -0.443$ as a function of $j$ for large values of $K/t$. To prove this point we show in the inset the nearest neighbors spin-spin correlation functions for a Heisenberg chain of the same size where the link at site zero is a factor of two smaller than the rest.
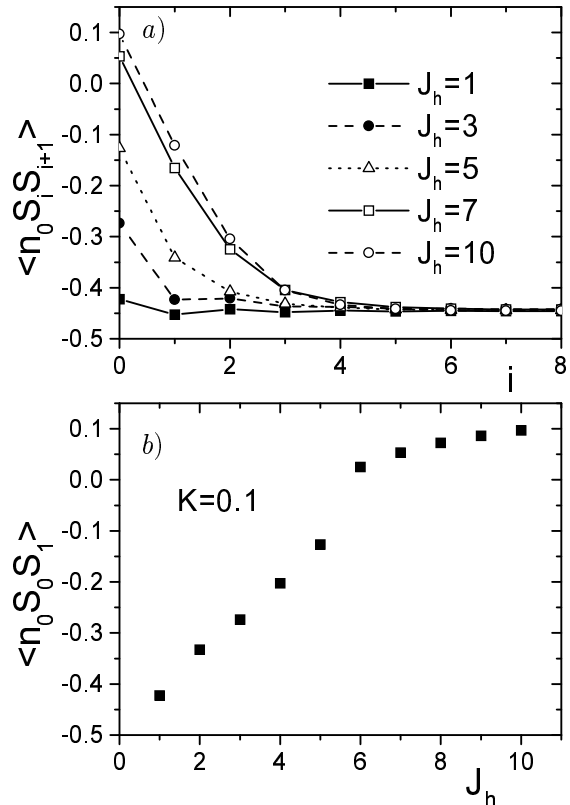


FIG. 2. *a*) Evolution of the polaron profile from the weak coupling regime ($J_h = 1$) to the strong coupling limit ($J_h = 10$). *b*) Magnetic correlation between the site where the particle is and the nearest neighbor as function of $J_h$.

In Fig.2(*b*) we show the variation of the polaron profile as a function of $J_h$, for $K/t = 0.1$. In this way it is possible to see the transition from non-polaronic (weak coupling) to polaronic (strong coupling ) regime.

### B. Dispersion relation

As K decreases, it is difficult to find an adequate approximation to describe the large polaronic distortion. In order to obtain the effective mass of these polarons, we investigate the dispersion relation for charge excitations. To this end we calculate the lowest energy state for different values of the momentum $k = 2\pi n/N$ within the subspace where the total spin is that of the ground state. In Fig.3 we show the dispersion relation scaled to the thermodynamic limit for $K = 3$, $J_h = 100$; $K = 1$, $J_h = 10$; and $K = 0.3$, $J_h = 10$.
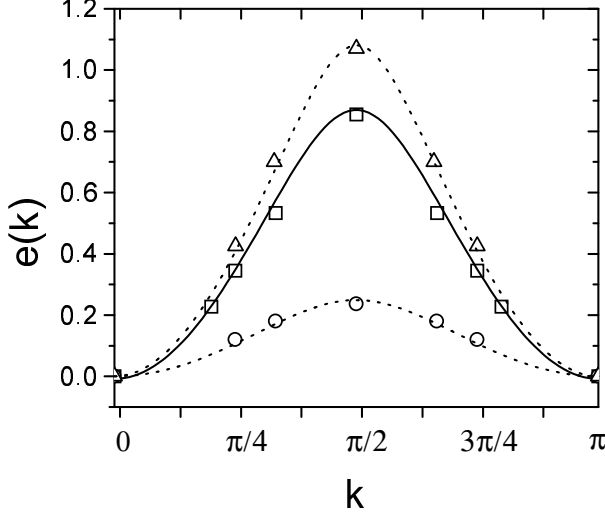
FIG. 3. Dispersion relation scaled to the thermodynamic limit for different sets of parameters. In full line we show a fit with the expression discussed in the text for the limit $J_H >> K > t$ with $\Delta = 1.4 \approx K/2$ (squares). In dotted line fit with $\Delta = 1$ and $t = 0.75$ for $K = 1$ (triangles) and $\Delta = 0.6$ and $t = 0.23$ for $K = 0.3$ (cicles).

We start analyzing the dynamics in the regime where $(J_h >> K >> t)$. In this case, the charge moves as a spin one ($\mathbf{\Sigma}$). The effective hopping resulting from the projection of the hopping term onto the reduced $S = 1$ Hilbert space is: $tP_{ij}(\mathbf{\Sigma}_i\mathbf{S}_j + 1/2)$, where $P_{ij}$ is the permutation operator between sites $i$ and $j$. We can picture the movement of the particle, in this limit, as going from a state $\downarrow \uparrow \downarrow \Uparrow \downarrow \uparrow \downarrow$ to an intermediate state $\downarrow \uparrow \downarrow \uparrow 0 \uparrow \downarrow$, and finally to $\downarrow \uparrow \downarrow \uparrow \downarrow \Uparrow \downarrow$, where $\Uparrow$ (0) represents the $S_z = +1(0)$ components of the spin $S = 1$. Thus, in order to move, the charge has to hop to the nearest neighbor, via a spin flip process, through states that differ in energy by $\Delta \approx K/2$. It can be easily verified that the effective hopping of this process is equal to $t_{ef} = t/\sqrt{2}$. The dispersion relation given by this dynamics is: $\Delta/2 \pm \sqrt{(\Delta/2)^2 + 4t_{ef}^2\cos^2(k)}$ . The expression corresponding to the lower band is plotted with full line in Fig.3 and compared with the numerical result for $K = 3$ and $J_h = 100$. This expression is valid in general for a particle moving in an antiferromagnetic background where scattering between $k$ and $k + \pi$ states dominates the dynamics of the particle (dotted lines in Fig.3).
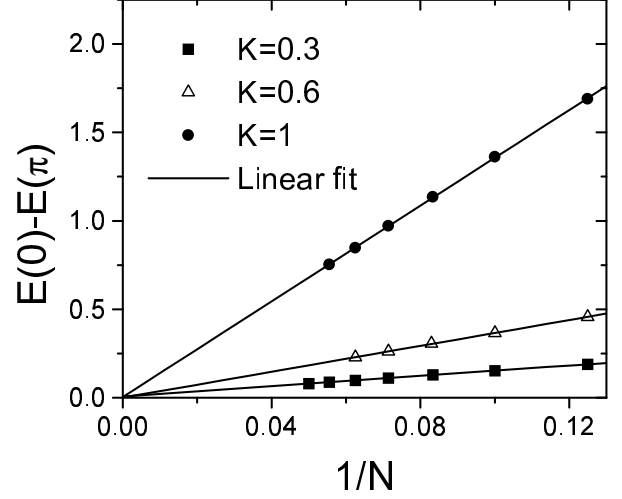


FIG. 4. Scaling of the difference between $k = 0$ and $k = \pi$ states for different values of $K$ and $J_h = 10$.

In Fig.4 we show the scaling of the energy difference between $k$ and $k + \pi$ states. This difference must tend to zero as $N$ tends to infinity due to the reasons explained above. In this way we can check the quality of the scaling used to calculate the points in Fig.3. The linear extrapolation goes to zero with an error lower than $5 \times 10^{-3}$ for the three values of $K/t$ considered.

In the case $K >> J_h >> t$ the spin distortion can be neglected and the particle propagates in an antiferromagnetic lattice. The Hund interaction alternates the site energy of the propagating particle so that the difference between the two sublattices is given by $\Delta = J_h(< \sigma_jS_{j+1} > - < \sigma_jS_j >) \cong J_h(< S_jS_{j+1} > - < \sigma_jS_j >)$ where we approximate $< \sigma_jS_j > \approx 1/4$ its value at the triplet state, and $< \sigma_jS_{j+1} > \approx < S_jS_{j+1} > = \ln 2 - 1/4$ , the Bethe ansatz value. Using these values we find $\Delta = 0.19J_h$. In this case $t_{ef}$ is equal to $t$.

When $J_h >> t \gtrsim K$, the magnetic distortion around the charge is large and the effective hopping is dominated by the overlap between the magnetic distortions about the nearest neighbors sites. This last effect dominates the polaron effective mass. Therefore, the mass of polarons increases when $K$ decreases, as obtained in Fig.3, where $t_{ef}$ decreases from 0.75 for $K = 1$ to 0.23 for $K = 0.3$, showing that the spin distortion around the charge increases in magnitude and extension when $K$ decreases.
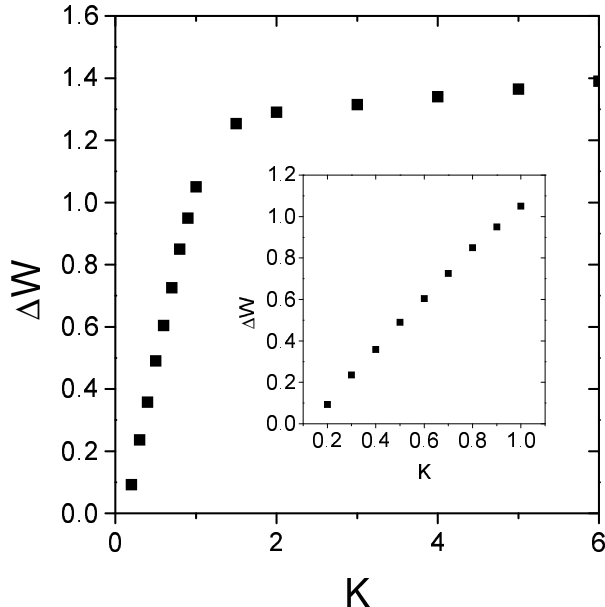
FIG. 5. Effective bandwidth as a function of $K$. The change of regime as $K/t$ increases is evident.

In Fig.5, we calculate the bandwidth for several values of $K$. Two regimes are clearly distinguished: $K \ll t$ and $K \gg t$. The first corresponds to a large magnetic distortion and the second corresponds to a smaller one according to Fig.1. The bandwidth goes to zero with $K$ indicating that the effective mass of the polaron increases continuously by decreasing $K$. When $K$ is equal to zero the size of the ferromagnetic distortion becomes infinite and we can not consider any more this distortion as part of the quasiparticle structure. The quasiparticle scenario is no longer valid (it is not possible to associate a magnetic distortion to the electron since the magnetic distortion is infinite). In this limit, the electron moves in a ferromagnetic background freely and thus generates a bandwidth equal to the tight-binding $4t$. In our case, since we are calculating finite systems, this happens for a small, but not zero, value of $K$. This regime is not shown in Fig.5.

### C. Localization

In order to test how robust is the polaronic description of the results, we pin the polaron by changing in $-\epsilon_0$ the diagonal energy at site zero. This may be relevant to the real materials since the doping process necessarily introduces some disorder. This always localizes the particle in a linear chain, but the localization length should be very different for different effective masses. A small $\epsilon_0$ localizes much more the polaron for low values of $K$ than for larger ones. This is shown in Fig.6(a) where we plot $< n_i >$ around site zero for different values of $K$, while

fixing $J_h = 10t$ and $\epsilon_0 = 0.05$. We also show in Fig.6(b) the correlation function $< n_0 S_j S_{j+1} >$ in order to determine the magnetic distortion associated with each localized state. While charge localization does not change very much for $K$ between 0.02 and 0.1, the magnetic distortion increases monotonically by decreasing $K$. To understand this point is useful to take the limit $K/t = 0$ and then slowly increment $K/t$. For $K/t = 0$, the system is a fully polarized ferromagnet and thus the ferromagnetic distortion is infinite. In this case, however, the localization length is finite, although the largest possible. As $K/t$ increases the magnetic distortion will shrink, without affecting the localization length, at least until they are comparable. In this regime the magnetic distortion is decreasing while the localization length is not changing. The difference between the localization and the magnetic distortion lengths depends on the value of $K$ and $\epsilon_0$, and determines the limit of validity of the quasiparticle concept.



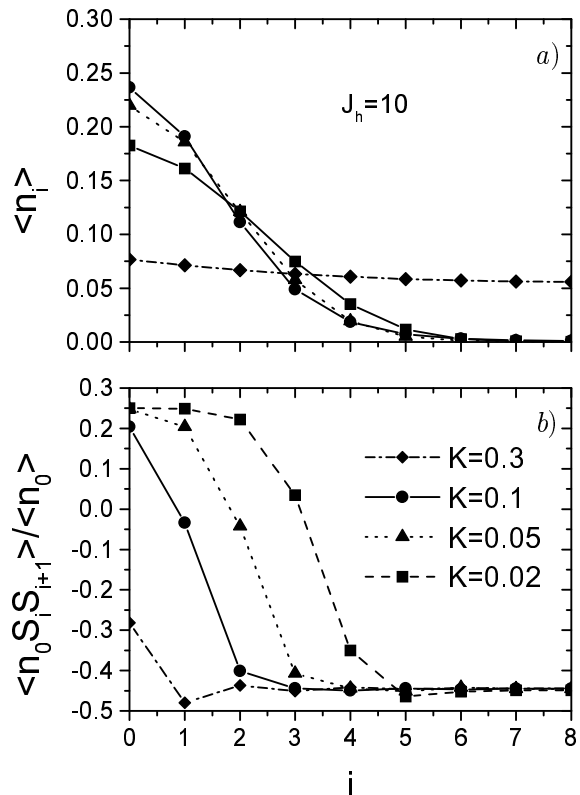FIG. 6. Charge localization. $a)$ We show $< n_i >$ as a function of position in a 16 sites chain where the energy at site zero is changed from the rest by $-\epsilon_0$=-0.05 units of $t$. The short localization length of the lower $K$ curves indicate effective bandwidths of the order of the energy change. $b)$ We show the extension of the magnetic distortion induced by the localized particle.

For large values of $K$ the polaronic distortion is very small and the localization length does not change substantially because the effective mass of the quasiparticle is similar to the free mass. When $K$ becomes smaller the localization length starts to decrease as a consequence of the increase of the effective mass. This behavior remains up to some value of $K$ where the size of the magnetic distortion is similar to the localization length. If we further decrease the value of $K$ then the localization length starts to increase up to the value corresponding to the free case for $K \ll \epsilon_0$, and we loose the quasiparticle picture.
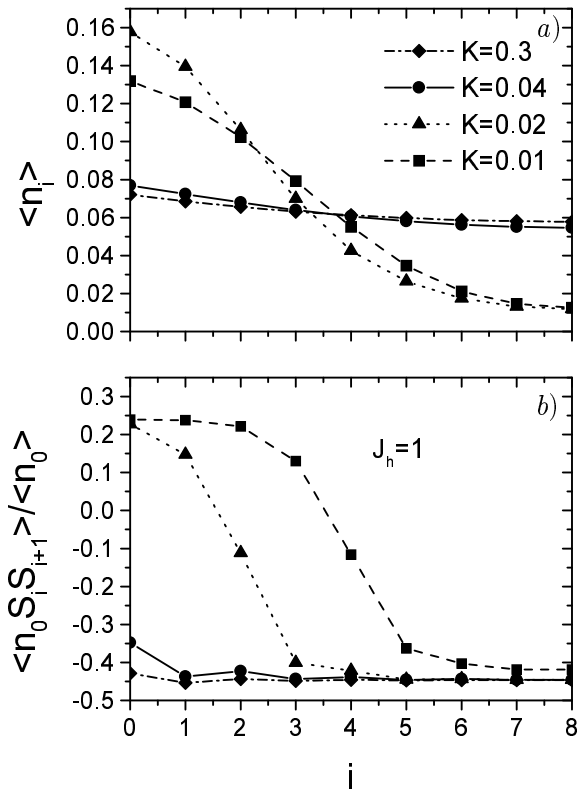


FIG. 7. Same as Fig.6 for the weak coupling regime ($J_h = 1$).

In Figs.7($a$) and ($b$) we show the same as in Fig.6 but for the weak coupling regime ($J_h = t$). In this case the localization length is always larger than in the strong coupling regime as expected. The size of the magnetic distortion is also smaller.
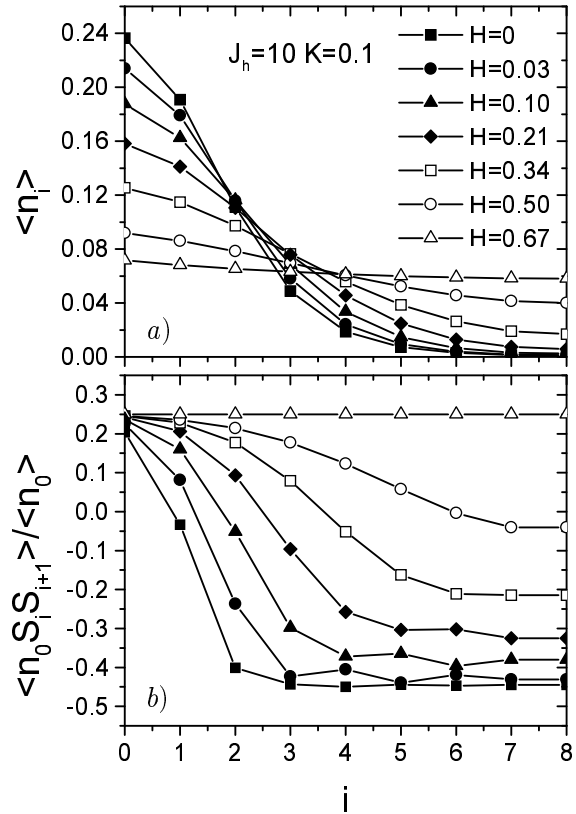


FIG. 8. Effect of magnetic field on charge localization in the strong coupling limit ($J_h = 10$). We show $a$) $< n_i >$ for different values of an external magnetic field for the same chain as in Fig.4; $b$) the evolution of the magnetic distortion as function of the magnetic field.

It is interesting to note the differences in the profile of the magnetic distortion between the localized case (Fig.6(a)) and the homogeneous case (Fig.1(a)). In the localized case the magnetic distortion is abrupt defining the polaron limits quite sharply (one could think of a step shape). In the non-localized case the polaron profile decays more continuously defocusing the polaron limits (one could think of an exponential-like shape).

In Fig 8($a$), we show the change in the values of $< n_i >$ for different magnetic fields in the strong coupling regime ($J_h = 10t$ and $K = 0.1t$). $S_z$ increases by one between two successive values of $H$ starting from $S_z = 2.5$ for $H = 0$. It can be seen that the localization of the polaron decreases with magnetic field as a consequence of increased effective hopping between nearest neighbors. A fact that may be important for the transport properties of these systems since it implies a negative magnetoresistive behavior for conductivity due to hopping between localized states [34,14,15]. The size of the magnetic distortion relative to the background increases with the magnetic field (see Fig.8(b)). This could be due to the stronger effect of the magnetic field on the spins which are close

to the boundary of the polaron. Those spins are forming weak links due to the competition between super and double exchange so they must have a larger susceptibility.
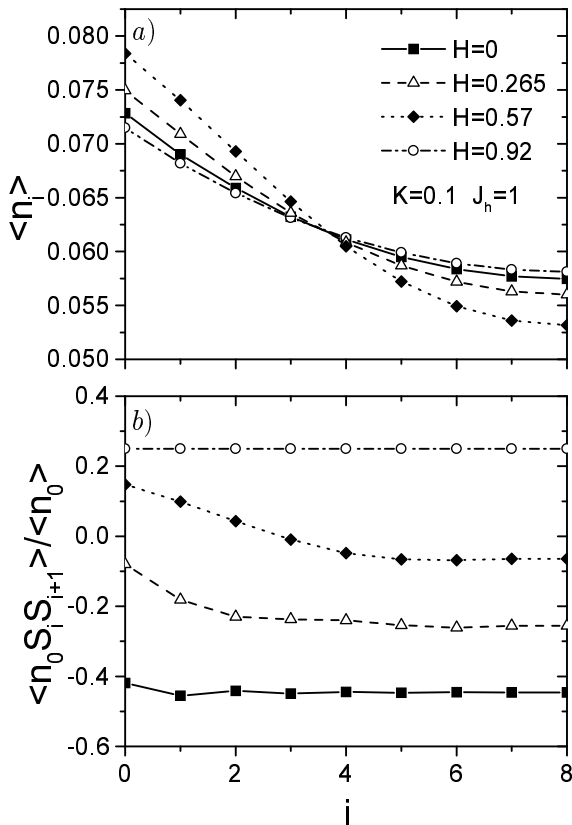


FIG. 9. The same as Fig.8 in the weak coupling limit ($J_h = 1$).

In Fig.9($a$) we show the effect of magnetic field on the localization for the weak coupling limit ($J_h = 1$, $K = 0.1$). It is clear from this figure that the magnetoresistive effect is very weak compared with the strong coupling limit. In addition, the size of the magnetic distortion is very small (Fig.9($b$)) as expected for the weak coupling regime.

## IV. TWO PARTICLES

In this section we study the interaction between the quasiparticles. To this end we calculate the magnetic distortion induced by two itinerant electrons, as well as the binding energy and the charge-charge correlation function. In this way it is possible to discriminate if the effective interaction is attractive or repulsive.
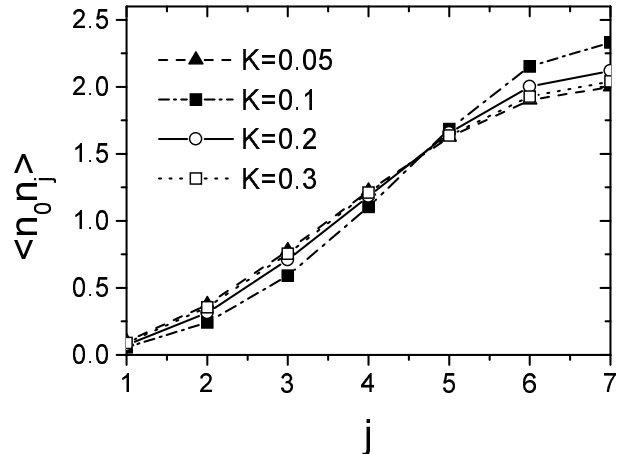


FIG. 10. Charge-charge correlation as a function of distance in the strong coupling limit ($J_h = 10$).

In order to obtain closed shell conditions in the spinless limit ($K/t = 0$ and $J_h \to \infty$) we have taken antiperiodic boundary conditions (APB). We have only used PBC for the calculation of binding energies because this quantity also involves the energy of one particle added, which has been calculated with PBC.

The charge-charge correlation function, $\langle n_0 n_j \rangle$ gives information about the character of the interaction between the polarons. This correlation function is shown in Fig.10 for a chain of 14 sites. The maximum always occurs for the largest possible distance between the particles, what could indicate a tendency towards repulsion. However in some cases this could just indicate that the size of the chain is similar or smaller than the mean separation between the two particles in a bound state. In order to discriminate between these two possibilities it is necessary to calculate the binding energy for different sizes of chains.
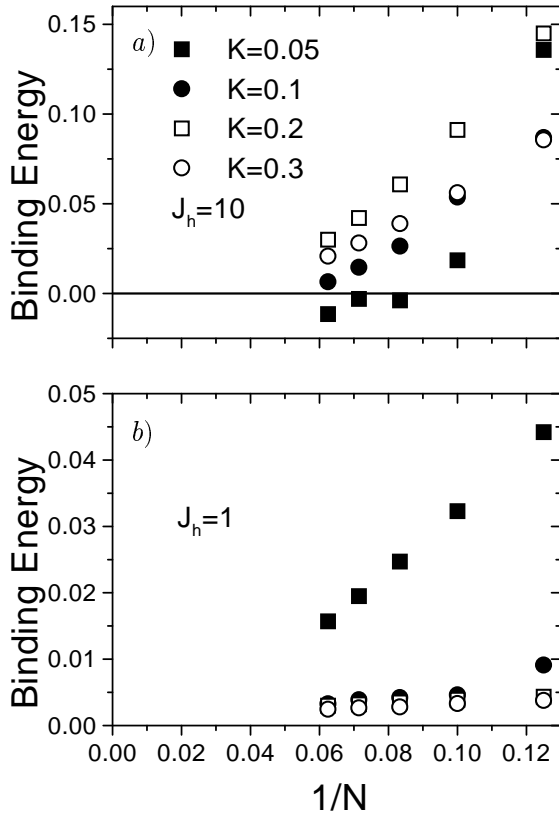
FIG. 11. Binding energy, $(E(2)+E(0)-2E(1))$, as function of the inverse of the system size in the strong coupling limit $(J_h = 10)$.

Fig.11$(a)$ shows the binding energy $(E(2) + E(0) - 2E(1))$ as a function of the inverse of the chain length, in the strong coupling limit. We find that, although up to the systems we can compute the interaction is always repulsive for $K \geq 0.1$, the extrapolation to the thermodynamic limit gives a negative value, indicating a bound state. When $K$ is low enough $(K = 0.05t)$ the binding energy is already negative for $N \geq 12$. The fact that the interaction is repulsive for chains smaller than 12 sites indicates that the mean separation of the bound pair is around six lattice parameters. In Fig.11(b) we show the weak coupling limit. Now for every value of $K$ we get a vanishing binding extrapolated to the thermodynamic limit. This reflects the importance of the double exchange in the dynamics of the electrons. By increasing the coupling the system crosses between a non-bounding regime into an attractive one.
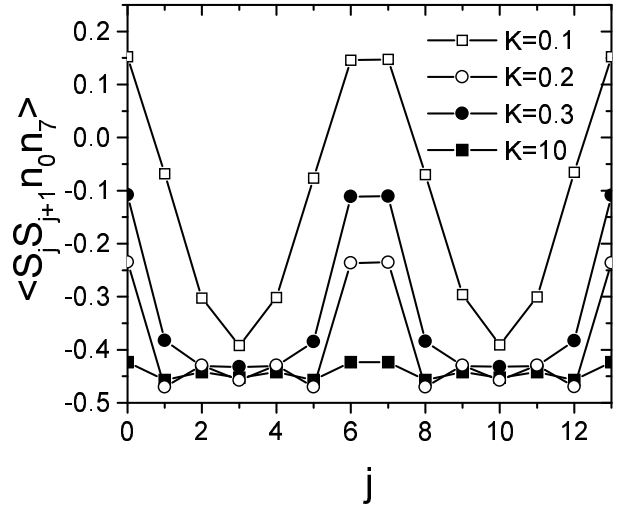


FIG. 12. Profile of the the magnetic distortion with two particles added for different values of $K$.

In Fig.12 we show the profile of the magnetic distortion for different values of $K$, for the maximum separation between the particles. As for the one particle case, the size and amplitude of the magnetic distortion increases as $K$ decrease giving rise to a strong polaronic regime for $K \sim 0.1t - 0.2t$. The two polarons are practically independent of each other, their shape being essentially the same as in the single polaron regime described in the previous section (see Fig.1). If the size of each polaron becomes larger than some critical length, one would expect that the second particle added could gain some magnetic energy by shearing the distortion created by the first one. This mechanism is similar to the spin-bag idea proposed by Schrieffer [33] to explain the attractive interaction giving rise to pairing in the high temperature superconductors. From this consideration, the existence of a bound state under some critical value of $K$ can be understood.
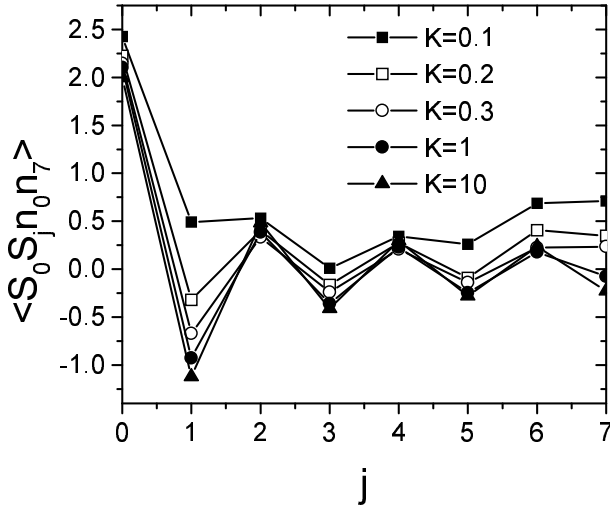
FIG. 13. Spin-spin correlation as function of distance for the largest separation between the charges.

If the spin-bag picture is correct, the polarons must interact ferromagnetically when they form a bound state. This can be checked by calculating the total spin of the ground state and the spin-spin correlation between the charges. In Fig.13 we show spin-spin correlation as a function of distance when one particle is at site zero and the other one is at the longest distance in the chain (site 7 in a 14 sites chain). It is clear that, as $K$ decreases, the interaction between the two charges becomes more ferromagnetic. To confirm this result, in Fig.14, we show the spin-spin correlation function between the two particles from where the effective magnetic interaction between the two quasiparticles can be extracted. It is clear that this interaction evolves from a very small value for $K = 0.4$ to the largest ferromagnetic value for $K = 0.1$.
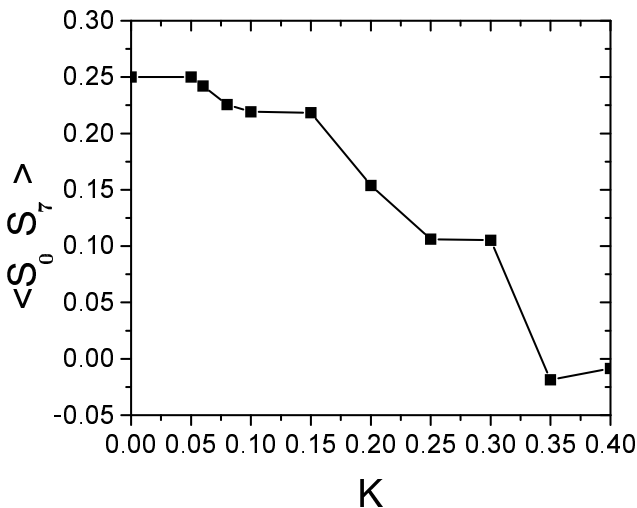


FIG. 14. Spin-spin correlation between the two added electrons for different values of $K$.

This change in the behavior of the interaction is also obtained in the charge-charge correlation function (Fig.10) where, for some critical value of $K$ between 0.1 and 0.05t, we observe a change in the variation of the intensity of the maximum with $K$. It increases with decreasing $K$ from 0.3 to 0.1 and then it decreases practically the same magnitude between $K = 0.1$ and $K = 0.05$.
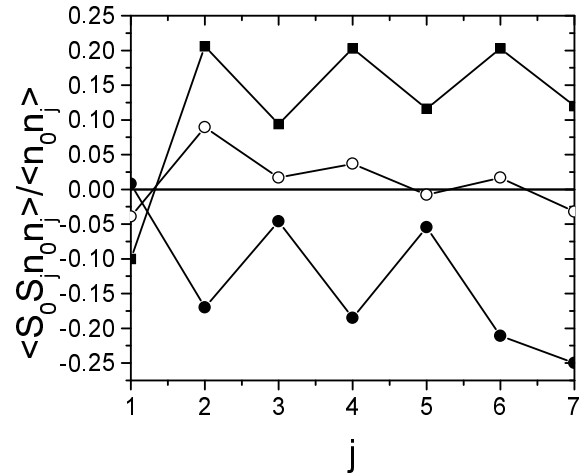


FIG. 15. Spin-spin correlation function between the two particles as function of the relative distance. The diagonal energies of sites 0 and 7 have been lowered by $\epsilon_0$ in order to pin the two quasiparticles for $K = 0.2$. $\epsilon_0 = 0.01$ (solid squares), $\epsilon_0 = 0.1$ (open circles), $\epsilon_0 = 1$ (solid circles).

We also studied interaction between polarons in the presence of disorder. As it is seen in Fig.6, the lowering of the diagonal energy of one site not only pins the quasiparticle, but also changes its size. This change should induce a modification of the effective magnetic interaction between two pinned quasiparticles. This can be seen in Fig.15 where we show the spin-spin correlation between the two particles a function of distance and for different values of $\epsilon_0$. The diagonal energy has been changed by $-\epsilon_0$ in both sites 0 and 7. The effective magnetic interaction evolves from ferromagnetic values for $\epsilon_0 < 0.1$ to antiferromagnetic for $\epsilon_0 > 0.1$. This can be easily understood from the reduction in the size of the polaron distortion which is induced by the increment of the pinning energy $\epsilon_0$. As each particle is more localized, the overlap between polaronic distortions decrease. Each particle cannot see the magnetic distortion generated by the other and the effective magnetic interaction is dominated by the superexchange through the localized spins between the two polarons.
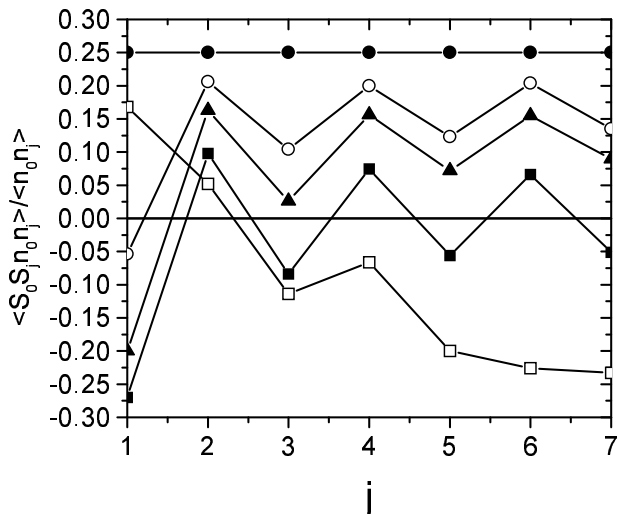
FIG. 16. Same as Fig.15, but for different values of $K$ and $\epsilon_0 = -0.05t$. $K = 0.05$ (solid circles), $K = 0.1$ (open squares), $K = 0.2$ (open circles), $K = 0.3$ (solid triangles), and $K = 0.5$ (solid squares).

In Fig.16, we show the variation of the effective magnetic interaction between two pinned quasiparticles as a function of $K$. In this case we get a non-monotonic behavior. By decreasing $K$ from 0.5 to 0.2 the effective interaction becomes more ferromagnetic. But for $K = 0.1$ this behavior changes drastically becoming antiferromagnetic when the particles are close to each other and ferromagnetic when each one is close to its pinning center. This indicates the formation of two well defined ferromagnetic distortions surrounding each center of pining with an antiferromagnetic effective interaction. For $K = 0.05$ this effective interaction becomes ferromagnetic and we get a uniform ferromagnetic state (the size of the induced distortion is equal to the size of the system).

Localizing the particle reduces the overlap between polarons, the system becomes more inhomogeneous and the effective interaction between the polarons evolves from ferromagnetic to antiferromagnetic. For example, for $K = 0.1 < S_0 S_7 n_0 n_7 >$ is positive for $\epsilon_0 = 0$ (Fig.13) and becomes negative for $\epsilon_0 = -0.05$ (Fig.16).

Finally we have studied how sensitive are the results to the inclusion of $U$ and $V$ in the strong coupling regime. We do not find any significant change in the physics due to the presence of these interactions. As we are studying the dilute limit, this interactions should not be so important as for higher concentrations. Even though, if both particles are at the same site, they must be in a singlet state due to the Pauli principle. This state has a very large energy ($\sim J_h$) in the strong coupling limit ($J_h = 10$) giving rise to a very small double occupation in the ground state. This explains the poor role of $U$. To explain the weak effect of $V$ it is useful to take a look at Fig.10 where it can be seen that the occupation of adjacent sites for the two particles is very small.

## V. CONCLUSIONS

In summary, we have investigated the possibility of a non uniform ground state in a model Hamiltonian using the Lanczos technique. The model describes chains of localized spins coupled antiferromagnetically and interacting ferromagnetically with itinerant electrons. We have studied in detail the case with one and two electrons. Assuming the model adequately describes the physics of electron doped manganites, the results presented here point to a picture of these systems where heavy polarons dominate the magnetic and transport properties. Their masses depend strongly on the relation between the hopping energy and the antiferromagnetic superexchange interaction. Clearly, the doping itself will localize the polarons so that transport will result from hopping between pinned sites. Negative magnetoresistance should appear as a consequence of the decrease of the pinning energy with magnetic field [34].

We have done scaling on the binding energy of two polarons. Two regimes can be identified depending on the coupling ($J_h$). In the strong coupling case, although only for small values of $K$ we find a negative binding ($K \leq 0.05$ and $N \geq 12$), the scaling to the thermodynamic limit is negative for every $K$ we have studied, indicating a bound state. In the weak coupling case, for most $K$ the scaling to the thermodynamic limit is zero, and all values are positive.

One possible way to induce a bound state is associated to the ferromagnetic distortion of the polarons. Below some critical value of $K$ this ferromagnetic distortion of two neighbor polarons overlaps and them the charge-charge interaction becomes attractive. This scheme resembles the spin-bag picture proposed by Schrieffer to explain the pairing mechanism in the High $T_c$ compounds. The effective magnetic interaction between polarons also changes from antiferromagnetic to ferromagnetic by decreasing the value of $K$.

We have also studied the effect of localization on the effective interaction between the quasiparticles. The effect of localization is not only to pin the quasiparticles but also to change the shape of the ferromagnetic distortion. As the shape and size of this distortion is clearly connected with the spin-spin and charge-charge effective interaction we get that the amount of disorder play a very relevant role in the low energy physics of these quasiparticles. Depending on the pining energies ferromagnetic and antiferromagnetic interactions could be generated. In real systems frustration induced by such competing interactions could give rise to spin glass behavior. In this way, the interplay between diagonal disorder and effective magnetic interactions between polarons could explain the cluster glass character of the metallic phase found by Maignan et. al. [19] in $Ca_{1-x}Sm_xMnO_3$ for $0 < x < 0.12$.

Finally, we would like to point out that the order of oxygen vacancies in $CaMnO_{3-\delta}$ makes real the possibility of one dimensional electron paths in these materials [35]. We hope that our results will stimulate more experimental and theoretical investigations on the electron doped manganites.

*Acknowledgments*

* Permanent address. LEPES is associated with Université Joseph Fourier, Grenoble.

[1] R. von Helmholt, J. Wecker, B. Holzapfel, L. Schultz, and K. Samwer, Phys. Rev. Lett. **71**, 2331 (1993).

[2] S. Jin, et al., Science **264**, 413 (1994), and rferences therein.

[3] Y. Tokura et al., J. Appl. Phys. **79** (8), 5289 (1996).

[4] A. P. Ramirez, J. of Physics: Condens. Matter 8171 (97), and references therein.

[5] J. M. D. Coey *et. al.*, Adv. Phys. **48**, 167 (1999).

[6] A.P. Ramirez *et. al.*, Phys. Rev. Lett. **76**, 3188 (1996).

[7] H. Kawano, R. Kajimoto, H. Yoshizawa, Y. Tomioka, H. Kuwahara, and Y. Tokura, Phys. Rev. Lett. **22,** 4253 (1997).

[8] H.L. Liu, S. L. Cooper, and S-W Cheong, Phys. Rev. Lett. **81**, 4684 (1998).

[9] W. Bao, J.D. Axe, C.H. Chen, and S-W. Cheong, Phys. Rev. Lett. **78**, 543 (1997).

[10] Y. Yamada et al.,Phys. Rev. Lett. **77,** 904 (1996).

[11] J. M. De Teresa et al., Nature (London) **386**, 256(1997).

[12] M.Hennion *et. al.*, Phys. Rev. Lett. **81**,1957 (1998).

[13] W. Bao et. al., Solid State Comm. **98**, 55 (1996).

[14] H. Chiba, M. Kikuchi, K. Kusaba, and Y. Syono, Solid State Commun. **99**, 499 (1996).

[15] I. O. Troyanchuk, N. V. Samsonenko, H. Szymczak, and A. Nabialek, Solid State Chem. **131**, 144 (1997).

[16] Y. Murakami, D. Shindo, H. Chiba, M. Kikuchi, K. Kusaba, and Y. Syono, Phys. Rev. B **55**, 15043 (1997).

[17] E. O. Wollan, and W. C. Koehler, Phys. Rev. 100, 545 (1955).

[18] P. Schiffer, A.P. Ramirez, W. Bao, and S-W Cheong, Phys. Rev. Lett. **75**, 3336 (1995).

[19] A. Maignan, C. Martin, B. Raveau, and J. Hejtmanek, Phys. Rev. B **58**, 2758 (1998).

[20] P. G. de Gennes, Phys. Rev. **118**, 141 (1960).

[21] D. P. Arovas and F. Guinea, Phys. Rev. B **58**, 9150 (1998).

[22] E. Dagotto *et. al.*, Phys. Rev. B **58**, 6414 (1998). ; J. Riera, K. Hallberg, and E. Dagotto, Phys. Rev. lett. **79**, 713 (1997); S. Yunoki *et. al.*, Phys. Rev. Lett. **80** 845 (1998).

[23] D.I.Golosov *et. al.*, J. Appl. Phys. **83** 7360 (1998); *ibid* Phys. Rev. B **58**, 8617 (1998).; H. Aliaga, R. Allub and B. Alascio., cond-mat/9804248

[24] M.Yu.Kagan, *et. al.*, cond-mat/9804213.

[25] M.R. Ibarra and J. M. De Teresa in "Transition Metal Oxides" Edt. C.N.R. Rao and B. Reveau, World Scientific (1998).

[26] S.Yunoki and A.Moreo, Phys. Rev. B **58**, 6403 (1998).

[27] A. L. Malvezzi, S. Yunoki, and E. Dagotto, cond-mat/9809281.

[28] Okimoto et. al., Phys.Rev. Lett. **75**, 109 (1995).

[29] Satpathy et. al., Phys.Rev. Lett. **76**, 960 (1996).

[30] Wei et. al., Phys.Rev. Lett. **79**, 5150 (1997).

[31] Jung et. al., Phys. Rev. B **55**, 15489 (1997).

[32] D.D. Sarma et. al., Phys. Rev. B **55** , 6873 (96)

[33] J. R. Schrieffer, X. C. Wen, S. C. Zhang, PRB **39**, 11663 (1989).

[34] Proceedings of the International Workshop on Current Problems in Condensed Matter Physics, Cocoyoc, Mexico. Plenum 1998

[35] J. Briatico, *et. al.* Phys. Rev. B **53**, 14020 (1996).